Remote Sensing of Environment 140 (2014) 155–164

Contents lists available at ScienceDirect

Remote Sensing of Environment

journal homepage: www.elsevier.com/locate/rse

Influence of atmospheric forcing and freshwater discharge on interannual variability of the vertical diffuse attenuation coefficient at 490 nm in the Baltic Sea

Malgorzata Stramska [a,b,*], Marek Świrgoń [b]

[a] Institute of Oceanology of the Polish Academy of Sciences, ul. Powstańców Warszawy 55, 81-712 Sopot, Poland
[b] University of Szczecin, Department of Earth Sciences, ul. Mickiewicza 16, 70-383 Szczecin, Poland

ARTICLE INFO

Article history:
Received 25 February 2013
Received in revised form 13 August 2013
Accepted 25 August 2013
Available online xxxx

Keywords:
Ocean color remote sensing
Diffuse attenuation coefficient
Baltic Sea
Interannual variability

ABSTRACT

Each year, spatial patterns of ocean color in the Baltic Sea differ in temporal evolution and magnitude. We have investigated the interannual variability of the spatially averaged vertical diffuse attenuation coefficient at 490 nm ($K_d(490)$) in response to atmospheric forcing and river discharge. Our results indicate that atmospheric forcing does not have a significant influence on interannual anomalies of $K_d(490)$ in the Baltic Sea. This is dissimilar to the North Atlantic at the same latitudes, where interannual variability of phytoplankton blooms (ocean color chlorophyll concentration, Chl, and K_d) is to a large degree controlled by local weather. In contrast, in the Baltic Sea the interannual variability of $K_d(490)$ is significantly influenced by river runoff. Higher values of $K_d(490)$ are observed in years with larger inflow of water from rivers. Without access to more detailed information about the concentrations of various optically significant water components we can only speculate about the possible reasons for this relationship. Most likely a combination of several factors causes the observed positive correlation between $K_d(490)$ and river discharge. These factors include development of more intense phytoplankton blooms in response to a larger supply of nutrients delivered by rivers. This conclusion is supported by satellite Chl data. However, an advection of optically important material with river water most likely also contributes to the bserved variability of $K_d(490)$. The diffuse attenuation coefficient plays a critical role in many oceanographic processes. For example, K_d is essential for quantification of radiative heating of the ocean, in models of primary production and other photoprocesses, and in studies discussing water turbidity and water quality. Better understanding of the variability of K_d in the Baltic Sea can improve our knowledge of this marine environment.
© 2013 Elsevier Inc. All rights reserved.

1. Introduction

To date most of the quantitative applications of ocean color remote sensing have focused on the determinations of abundance of phytoplankton chlorophyll in the world's oceans. Global ocean color bio-optical algorithms have also been used to relate the remote sensing reflectance (R_{rs}) to the concentrations and optical properties of other seawater constituents in the open ocean regions. Such interpretation presents more difficulty in optically complex waters (but see for example Fichot et al., 2013). Optically complex waters (i.e. Case-2 waters) exhibit a general lack of correlation between concentrations of optically significant constituents (as opposed to Case-1 waters, see Gordon & Morel, 1983; Morel, 1988). Although Case-2 waters cover a small fraction of the global ocean, they include many coastal regions of great social, economic and ecological importance (IOCCG, 2000). One example of such an optically challenging region is the Baltic Sea.

It has been shown in the past that, in the Baltic Sea, the best performance among all standard ocean color algorithms is achieved with the algorithm for the diffuse attenuation coefficient for downwelling irradiance (K_d). The average of absolute percentage difference between the in situ measured and the semianalytically derived $K_d(\lambda)$ was 14% for $\lambda = 490$ nm and 11% for $\lambda = 443$ nm (Lee, Darecki, Carder, Davis, Stramski, & Rhea, 2005). The spectral vertical attenuation of downwelling irradiance, $K_d(\lambda, z)$, is defined as:

$$K_d(\lambda, z) = -\mathrm{d}\ln[E_d(\lambda, z)]/\mathrm{d}z \quad (1)$$

where $E_d(\lambda, z)$ is the planar downwelling irradiance, z is the water depth, and λ is the light wavelength in vacuum. Strictly speaking, $K_d(\lambda, z)$ is not a property of the water itself, but rather a descriptor of the underwater light field. It varies with depth and solar altitude (e.g. Mobley, 1994; Stramska & Frye, 1997). For simplicity, in the equations, we will omit the dependence of the optical properties on water depth. In many studies $K_d(\lambda)$ has been treated as a quasi-inherent optical property (quasi-IOP), because experimental data and inverse radiative transfer modeling efforts have shown that

* Corresponding author. Tel.: +48 58 73 11 600; fax: +48 58 55 12 130.
E-mail addresses: mstramska@iopan.gda.pl, mstramska@wp.pl (M. Stramska).

0034-4257/$ – see front matter © 2013 Elsevier Inc. All rights reserved.
http://dx.doi.org/10.1016/j.rse.2013.08.043

$K_d(\lambda)$ is strongly correlated with inherent optical properties, IOPs (see Kirk, 1984, 1991; Mobley, 1994; Stramska, Stramski, Mitchell, & Mobley, 2000). For example, $K_d(\lambda)$ can be approximated as:

$$K_d(\lambda) \sim a(\lambda) + b_b(\lambda) \quad (2)$$

where $a(\lambda)$ is the total absorption coefficient and $b_b(\lambda)$ is the backscattering coefficient of seawater. Thus, in waters with a high a/b_b ratio such as the Baltic Sea, the variability of $K_d(\lambda)$ can be expected to be closely related to the variability of the total absorption coefficient, $a(\lambda)$. The $a(\lambda)$ coefficient is often partitioned into four additive components associated with broadly defined categories of seawater constituents (e.g., Mobley, 1994):

$$a(\lambda) = a_w(\lambda) + a_{ph}(\lambda) + a_{NAP}(\lambda) + a_{CDOM}(\lambda) \quad (3)$$

where the subscript w denotes the pure seawater, ph the phytoplankton, NAP the nonalgal particles suspended in seawater (this component includes non-living organic and mineral particles, and heterotrophic organisms), and CDOM is the colored dissolved organic matter or chromophoric dissolved organic matter. (In general, a_{CDOM} is operationally defined as the absorption coefficient of the material that passes through a 0.2 μm pore filter, see Nelson & Siegel, 2002.) Because CDOM and nonalgal particles (NAP) are characterized by similar exponentially decreasing absorption spectrum with increasing wavelength (Bricaud, Morel, & Prieur, 1981; Roesler, Perry, & Carder, 1989), some ocean color algorithms combine them into a colored detrital material with a unique absorption coefficient referred to as a_{CDM} (see Siegel, Doney, & Yoder, 2002):

$$a_{CDM} = a_{CDOM} + a_{NAP}. \quad (4)$$

In this paper, we present results from an analysis of the year-to-year variability of spatially averaged $K_d(490)$ in the Baltic Sea during the spring–summer months. Our analysis is based on SeaWiFS-derived data covering 13 years (1998–2010). We have compared interannual variability of spatially averaged $K_d(490)$ with patterns in local weather and variability in river runoff. Our main goal is to investigate what are the most important environmental factors forcing the interannual variability of the diffuse attenuation coefficient in the Baltic Sea. Note, that the diffuse attenuation coefficient for solar downward irradiance plays a critical role in many oceanographic research problems. For example, K_d has to be taken into account in parameterizations of radiative heating of the ocean (e.g., Mobley & Boss, 2012; Stramska & Dickey, 1993; Stramska & Zuzewicz, 2013; Zaneveld, Kitchen, & Pak, 1981), in models of primary production (e.g., Friedrichs et al., 2009; Wozniak et al., 2008), and is used in studies considering water quality. An analysis of the interannual variability of $K_d(490)$ in the Baltic Sea, which is the main focus of this paper, can lead to better understanding of this marine environment. The Baltic Sea is one of the largest brackish water systems of the world. It is surrounded by nine countries with more than 85 million inhabitants, and it experiences problems due to increasing anthropogenic eutrophication (HELCOM., 2009). It is therefore important to improve our understanding of the dynamic connections of this marine system with external forcing in order to derive a better understanding of the possible cause–effect relationships among different environmental variables and future trends.

2. Regional conditions

The Baltic Sea is a semienclosed sea located in Northern Europe (about 53°N to 66°N and 20°E to 26°E). Its volume is about 21 205 km^3 (Leppäranta & Myrberg, 2009). Annually about 480 km^3 of freshwater is added to the Baltic Sea by river runoff and atmospheric net flux (precipitation minus evaporation). The net atmospheric input is about one order of magnitude smaller than the river input. The drainage basin of the Baltic Sea has a surface area of about 1.633 10^6 km^2 that is about 4.2 times the area of the sea basin. The annual river inflow into the Baltic Sea (without the Danish Straits) is about 440 km^3 (Bergstrom & Carlsson, 1994; Mikulski, 1985). This amount of water corresponds to a layer of water of about 1170 mm if spreads over the entire Baltic Sea surface. River runoff undergoes temporal variations on time scales from years to decades, with the smallest annual inflow of 350 km^3 recorded in 1924 and the largest annual inflow of 615 km^3 recorded in 1976 (Leppäranta & Myrberg, 2009). Generally, the timing of the annual maximum in runoff happens later in the north than in the south, due to the timing of the snowmelt. For example, annual maximum in river runoff is observed in April in the central Baltic and in May–June in the Gulf of Finland. The river discharge is of great importance not only for the Baltic Sea, but also has significant influence on the hydrography of the North and Norwegian Seas (Leppäranta & Myrberg, 2009). Significant influx of freshwater from rivers promotes a permanent two-layer salinity structure in the Baltic Sea with a persistent halocline and an estuarine-like water exchange with the North Sea. The intensity of the inflow and outflow of water depends on the sea-level difference between the Baltic Sea and the North Sea and on weather patterns (e.g., Omstedt, Elken, Lehmann, & Piechura, 2004).

The depth of the Baltic Sea permanent halocline varies between 40 and 80 m (Leppäranta & Myrberg, 2009). A seasonal surface layer with relatively warm and low salinity waters is embedded in the upper layer of the Baltic Sea waters. This seasonal layer is formed in the spring due to seasonally increased freshwater input and solar heating. During recent decades, chlorophyll-a concentrations have been increasing in most of the Baltic Sea sub-regions. This has been caused by substantial inputs of nutrients into the Baltic Sea. As a result phytoplankton biomass and water turbidity increased while light penetration depth through the water column decreased. This process of eutrophication of the Baltic Sea resulted in many negative effects on the status of this marine environment, for example changes in the dominance of various phytoplankton functional groups including more frequent cyanobacterial blooms reduced colonization depth of macroalgae and seagrasses, increased sedimentation of organic matter to the seabed, oxygen depletion in the sediments and bottom water, and loss of benthic animals and fish (e.g., Håkanson & Bryhn, 2008; HELCOM., 2009).

The optical properties of the Baltic Sea waters are dominated by the presence of relatively high content of organic matter in the total suspended matter (TSM) as well as in the dissolved phase. Babin et al. (2003) investigated suspended particulate matter of various marine European coastal waters and found that the Baltic Sea is characterized by the highest contribution (~40%) of the particulate organic carbon (POC) to the TSM among the regions investigated. Babin et al. (2003) emphasized that the POC contribution to the TSM in the Baltic Sea is of the same order as in major European rivers. The contribution of particulate inorganic carbon (PIC) was about 10%, which is similar to the open ocean waters. The absorption budget derived for the Baltic Sea by Babin et al. (2003) indicates that CDOM absorption contributes about 50% of a–a_w at 443 nm, and slightly less at 490 nm. Importantly, according to Babin et al. (2003) the slope of the exponential function describing CDOM absorption in the Baltic Sea shows little variability and is similar to that in the Atlantic Ocean. In addition, Babin et al. (2003) observed weak variations in the exponential slope of NAP absorption. This suggests that although the concentrations of suspended and colored dissolved organic matter in the Baltic Sea are relatively high, the specific absorbing properties of these water components are similar to those observed in other ocean regions. Relatively high concentrations of suspended and dissolved organic matter in the Baltic Sea are associated with the fact that it is an intercontinental shallow marine environment, under strong influence of human activities and terrestrial material.

In order to better emphasize the regional features in the variability of ocean color in the Baltic Sea we will make comparisons with the North Atlantic Ocean. Open Atlantic waters belong to the Case 1 optical water

type. In Case 1 waters, the variability in ocean color is significantly correlated with surface chlorophyll concentration, Chl (e.g. Mobley, 1994). The annual patterns of the variability of Chl and the vertical diffuse attenuation coefficient in the North Atlantic generally follow the major phases of regional phytoplankton blooms (e.g., Gregg, 2002). These phases can be summarized as follows (Ducklow & Harris, 1993; Reid, Colebrook, Matthews, & Aiken, 2003; Siegel, Maritorena, Nelson, Hansell, & Lorenzi-Kayser, 2002). In early spring, there is a good supply of nutrients in the North Atlantic waters and at the top of the water column there may be high illumination, but phytoplankton are mixed and do not remain long enough near the surface to receive adequate light energy for significant growth. With the progression of seasonal stratification through the spring and early summer, there are enough nutrients and light to support phytoplankton growth and for the blooms to build on. Zooplankton grazing also becomes considerable. During this time of the year, periodic events of increased mixing due to storm passage result in the removal of a significant portion of the biomass out of the surface waters and replace nutrients (Marra, Bidigare, & Dickey, 1990; Martin et al., 2011; Stramska et al., 1995). Finally, later in the season there is enough light but not enough nutrients to support growth, and phytoplankton biomass decreases. In the fall, intermittent mixing due to storms and a seasonal decrease in water stratification may restock nutrients and bring about a secondary phytoplankton bloom. This simplified phytoplankton bloom scenario briefly described here demonstrates that the progression of seasonal stratification of oceanic surface waters forced by ocean–atmosphere interactions has a crucial influence on phytoplankton dynamics in this region. In agreement with this scenario, it has been observed that the interannual variability of phytoplankton concentration in the North Atlantic is significantly correlated with meteorological forcing (e.g., Dutkiewicz, Follows, Marshall, & Gregg, 2001; Follows & Dutkiewicz, 2002; Stramska, 2005; Stramska & Dickey, 1994; Stramska et al., 1995). The links between the biological productivity and environmental conditions have been discussed in oceanography for a long time (e.g., Doney, Glover, & Najjar, 1996; Fasham, Ducklow, & McKelvie, 1990; Gregg, 2002; Marra, 2004; Marra & Ho, 1993; Neumann, Fennel, & Kremp, 2002; Riley, Stommel, & Bumpus, 1949; Siegel, Maritorena et al., 2002; Smetacek & Passow, 1990; Sverdrup, 1953). It is very striking that even models with relatively simple theoretical treatment of biological processes are able to reproduce many important aspects of phytoplankton dynamics in the ocean and stress the important role of atmospheric forcing.

3. Data sources and methods

This study is based on satellite-derived ocean color data and meteorological and hydrographic data from various historical databases. Our main focus is the Baltic Sea. For comparison we also used similar data sets for the open ocean site located in the North Atlantic at the same geographical latitude as the Baltic Sea. The primary data sets, ocean color data products K_d_Lee(490) and Chl_GSM from SeaWiFS (e.g., Hooker & McClain, 2000), cover 13 successive years (1998–2010). The standard data processing procedures applied by NASA to derive a range of geophysical data products involve atmospheric correction and removal of pixels with land, ice, clouds, or heavy aerosol load prior to calculation of ocean color data products. Our analysis is based on Level 3 data, which were binned on an equal-area grid with a nominal 9 km × 9 km resolution (reprocessing version 2012). These data were obtained from NASA's Ocean Color Web (www.oceancolor.gsfc.nasa.gov/). We used monthly composites because of the significant loss of data due to cloud cover in the daily composites at the latitudes used in our study. In the text the terms such as "SeaWiFS monthly Chl composite for the month of May" will be interchangeably referred to as "monthly Chl" or "May Chl." The data were spatially averaged over the study region located in the central part of the Baltic Proper as shown in Fig. 1. Sensitivity tests have shown that the results presented below generally do not depend on the exact dimensions of the study

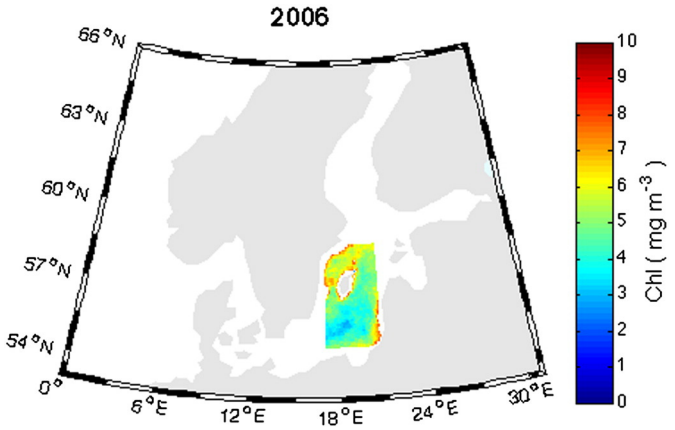

Fig. 1. Location of our study area in the Baltic Sea. Color scale indicates annual concentration of surface chlorophyll (Chl) derived from SeaWiFS data in 2006. (For interpretation of the references to color in this figure legend, the reader is referred to the web version of this article.)

area. In the North Atlantic, the region of interest is centered at 56°N 20°W and the data were averaged in the box of approximately 2° × 2° (Fig. 2).

A potential source of uncertainty in our results is the fact that ocean color data used in this study are based on global algorithms, rather than regional algorithms. This is not a problem in open ocean regions, such as the North Atlantic. However, the Baltic Sea waters are optically classified as Case 2 waters due to typically high CDOM and suspended matter concentrations (Babin et al., 2003; Kowalczuk, Stedmon, & Markager, 2006). In Case 2 waters the standard NASA algorithms generally do not perform well. Nevertheless, as mentioned before, a comparison of the vertical attenuation coefficient K_d derived from satellite data with in situ data showed an adequate performance of the K_d ocean color product in the Baltic Sea (Lee, Darecki, et al., 2005). Therefore, our results for the Baltic Sea are mostly presented for the global satellite K_d_Lee(490) product. For comparison we also present some results using the surface chlorophyll *a* concentration (Chl, mg m^{-3}) derived from GSM01 algorithm (e.g., Maritorena & Siegel, 2005; Maritorena, Siegel, & Peterson, 2002). The GSM Chl data product has been shown to correlate positively with in situ Chl determinations in the Baltic Sea (Coppini et al., 2012). In addition, for comparison, we have decided to use the particulate backscattering coefficient $b_{bp}(443)$ provided by NASA. The $b_{bp}(443)$ has been derived with the same algorithm as

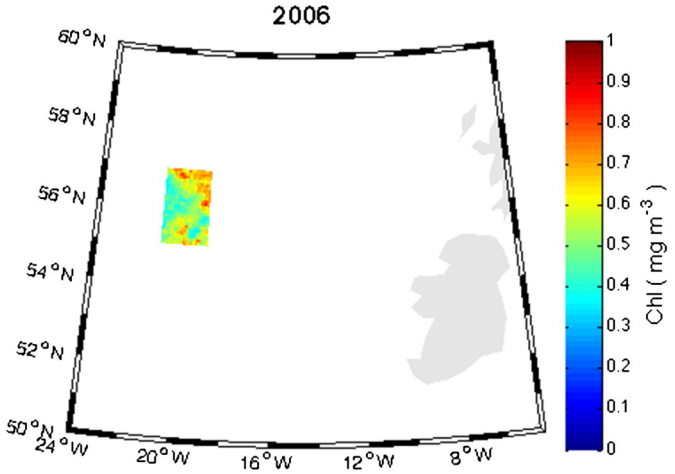

Fig. 2. Location of the site in the North Atlantic, used for comparison with the Baltic Sea data. Color scale indicates annual concentration of surface chlorophyll (Chl) derived from SeaWiFS data in 2006. (For interpretation of the references to color in this figure legend, the reader is referred to the web version of this article.)

K_d_Lee(490) (QAA algorithm, Lee, Darecki, et al., 2005; Lee, Du, & Arnone, 2005; Lee et al., 2007). The IOPs derived with the QAA algorithm have been validated in a wide range of oceanic and coastal conditions including Case 1 and Case 2 waters (e.g., Doron, Babin, Mangin, & Hembise, 2007; Lee, Darecki, et al., 2005, Lee et al., 2007). The QAA was the best algorithm for the retrieval of the a and b_b according to the IOCCG (2006).

To evaluate atmospheric forcing, we used meteorological data from the NOAA–CIRES Climate Diagnostic Center NCEP/NCAR (National Centers for Environmental Prediction and National Center for Atmospheric Research) Reanalysis Project, which applies a state-of-the-art analysis/forecast system to assimilate global meteorological data from various available sources (including satellite data) from 1948 to the present. In particular, we have utilized the latent and sensible heat flux estimates, along with the net longwave and net shortwave radiation estimates, to calculate the net heat flux H_0 at the sea surface. We have also used the wind stress data.

To investigate if atmospheric forcing can be linked to interannual variability of water optical properties we have applied the bulk mixed layer theory (Kraus & Turner, 1967; Niiler & Kraus, 1977; see also Follows & Dutkiewicz, 2002). Accordingly, the vertical mixing of water properties in the vertically homogenous oceanic mixed layer has been related to the rate of generation of turbulent kinetic energy (TKE_{RT}). The TKE_{RT} has been quantified in terms of wind stirring and buoyancy forcing:

$$TKE_{RT} = \int_h^0 \frac{d(TKE)}{dt} = m_1 u_*^3 + m_2 \frac{\alpha g}{\rho c_p} \frac{MLD}{2} H_0 \quad (5)$$

where TKE is the turbulent kinetic energy, MLD is the mixed layer depth, u_* is the wind-induced friction velocity, ρ is the water density, c_p is the specific heat, g is the gravitational acceleration, α is the coefficient of logarithmic expansion of ρ as a function of water temperature, and H_0 is the net heat flux. The coefficients m_1 and m_2 are difficult to quantify, though several authors (e.g., Kraus, Bleck, & Hanson, 1988) have assumed $m_1 = 1.25$ and $m_2 = 1$ for negative buoyancy forcing (heat loss from the surface ocean) and $m_2 = 0.2$ for positive buoyancy forcing (surface ocean gains heat). We have used these values for the m_1 and m_2 coefficients. Eq. 5 estimates the TKE_{RT} with the assumption that effects due to internal waves, energy dissipation, and variable vertical distribution of penetrative radiation with water turbidity are small and can be neglected. The first term on the right-hand side of Eq. 5 ($m_1 u^3$) indicates the rate of work by the wind. The second term on the right-hand side of Eq. 5 $\left(m_2 \frac{\alpha g}{\rho c_p} \frac{MLD}{2} H_0\right)$ represents the rate of potential energy change produced by heat fluxes. Note that the wind action always increases TKE_{RT} in the oceanic boundary layer. The buoyancy forcing can either increase TKE_{RT} when the water column is cooled from above ($H_0 > 0$), or reduce TKE_{RT} when the water column is stratifying due to heat input to the surface ocean from the atmosphere ($H_0 < 0$). Another environmental parameter needed for calculation of TKE_{RT} was the oceanic mixed layer depth (MLD). For our calculations we have used monthly climatological MLD data from de Boyer Montégut, Madec, Fischer, Lazar, and Iudicone (2004) (data at www.ifremer.fr/cerweb/deboyer/mld/home.php). These MLD estimates are based on extensive in situ data sets. In particular we have checked that these MLD data are in agreement with other published estimates of MLD in the Baltic Sea (Fu, She, & Dobrynin, 2012; Leppäranta & Myrberg, 2009). In addition, we have verified that the conclusions from our correlational analysis remain virtually unchanged if the MLD values are assumed to differ by +/− 20% from de Boyer Montégut et al. (2004).

River data for the Baltic Sea basin were taken from the HYPE model for water and nutrient runoff (model Balt-HYPE, data at www.balt-hypeweb.smhi.se) set up in the Swedish Meteorological and Hydrological Institute (SMHI). The model has been calibrated against daily observed values of river runoff in the framework of BALTEX (The Baltic Sea Experiment) and GRDC (the Global Runoff Data Centre) using a number of representative gauged basin upstream and at the river outlets (Donnelly, Strömqvist, & Arheimer, 2011). For our analysis we have used the reconstruction of historic discharge and nutrients at daily time-step in years 1998 to 2008. After 2008 such data were not available.

Because there is a strong seasonal variability in the data sets used in this study, we have chosen to independently analyze the data representing different parts of the seasonal cycle. Therefore, to evaluate the interannual variability, we will separately compare data from different months. All of the results from the statistical analysis included in the Results sections are statistically significant ($p < 0.05$, 95% confidence level).

4. Results

4.1. Relationship between atmospheric forcing and ocean color products

Summaries of meteorological data for the Baltic Sea and the North Atlantic sites are presented in Figs. 3 and 4, respectively, as the 13-year averaged (1998–2010) time series of daily estimates of the wind stress magnitude, net heat flux, and TKE_{RT}. The 13-year averaged monthly means of these quantities are indicated as the horizontal lines for the month of April through September, i.e. for the part of the calendar year discussed in this paper. From a comparison of Figs. 3 and 4 it is clear that the Atlantic site is exposed to a wider range of wind stress and heat flux values over the year than the Baltic Sea site. In particular, significantly larger values of TKE_{RT} in the Atlantic site are observed during the winter. In both regions, the net heat flux is positive in the winter indicating a cooling of the sea surface (in our paper a positive sign means that the heat flux is directed from the ocean into the atmosphere). In the Baltic Sea, the net heat flux becomes negative in April, when the seasonal heating of surface waters becomes significant due to the seasonal increase in solar radiation. The 13-year averaged monthly means of the net heat flux in the Baltic Sea remain negative from April to August, which is indicative of persistent warming of the sea. Thus, during this phase of the annual cycle the net heat flux in the Baltic Sea reduces the TKE_{RT} generated by the wind action. The seasonal minimum of TKE_{RT} is generally observed in the Baltic Sea in May–July (due to the significant heating of the sea and low wind stress). In contrast, in the

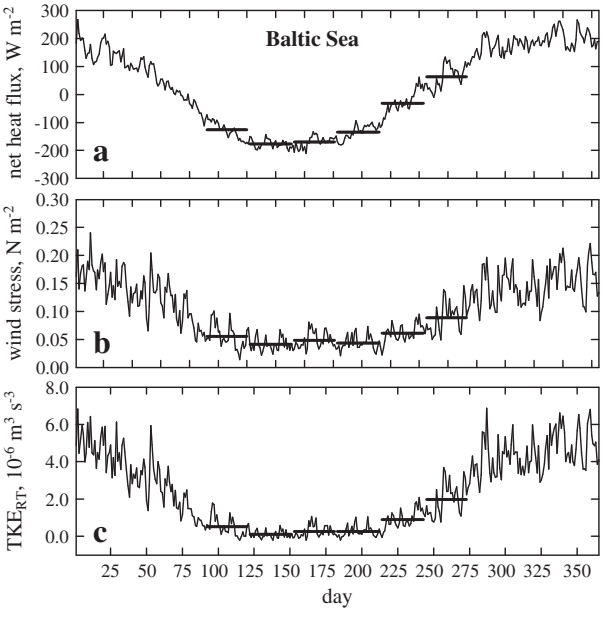

Fig. 3. The 13-year averaged daily means (solid line) of the (a) net heat flux, (b) wind stress magnitude, and (c) turbulent energy generation rate (TKE_{RT}) in the Baltic Sea based on the NCEP data. Horizontal lines indicate monthly averaged data in April through September.

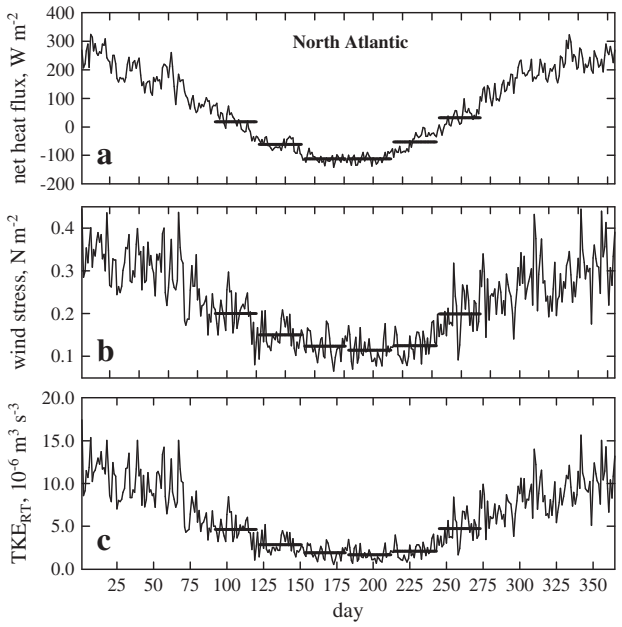

Fig. 4. The 13-year averaged daily means (solid line) of the (a) net heat flux, (b) wind stress magnitude, and (c) turbulent energy generation rate (TKE_{RT}) in the North Atlantic site based on the NCEP data. Horizontal lines indicate monthly averaged data in April through September.

Atlantic site, the annual cycle of the net heat flux and wind stress leads to a minimum in the TKE_{RT} in the months of June–August, which is somewhat later than in the Baltic Sea. The entire 13-year time series of wind stress magnitude and net heat flux discussed in this paper are presented in Figs. 5 and 6 for the Baltic Sea and North Atlantic sites, respectively. These data indicate that we did not observe any significant trend in the atmospheric forcing during the time period discussed here, although some interannual variability is evident in the data. Interannual variability is also illustrated with the monthly anomalies of wind stress and net heat flux shown in the bottom panels in Figs. 5 and 6.

Time series of monthly composites of $K_d(490)$ estimated with the Lee, Darecki, et al. (2005), Lee, Du, et al. (2005) algorithm and averaged over the study area in the Baltic Sea are plotted in Fig. 7a. Recall that the variability of K_d is influenced by the combined effect from major optically significant components of the water i.e. CDOM, phytoplankton, and NAP concentrations. For comparison, similar time series based on the monthly composites of chlorophyll concentrations estimated with GSM01 algorithm are also shown in Fig. 7a. Time series of $K_d(490)$ and Chl shown in Fig. 7a display an annual cycle of variability with larger values in late spring/summer seasons. Corresponding time series of monthly composites of $K_d(490)$ and Chl concentration derived for the North Atlantic site are displayed in Fig. 7b. Note, that the data from the North Atlantic site are characterized by significantly lower values of $K_d(490)$ and Chl than the data from the Baltic Sea. In addition, the annual cycle in the bio-optical data is more pronounced in the North Atlantic ocean, because both the $K_d(490)$ and Chl drop to very low values in late winter and early spring and are characterized by a prominent increase in the spring/summer seasons due to phytoplankton blooms. There is a significant interannual variability in the magnitude of these blooms. In April, during the initial period of bloom development, Chl is still relatively low. In May and June an increased surface irradiance and mixed layer shoaling associated with low values of TKE_{RT},

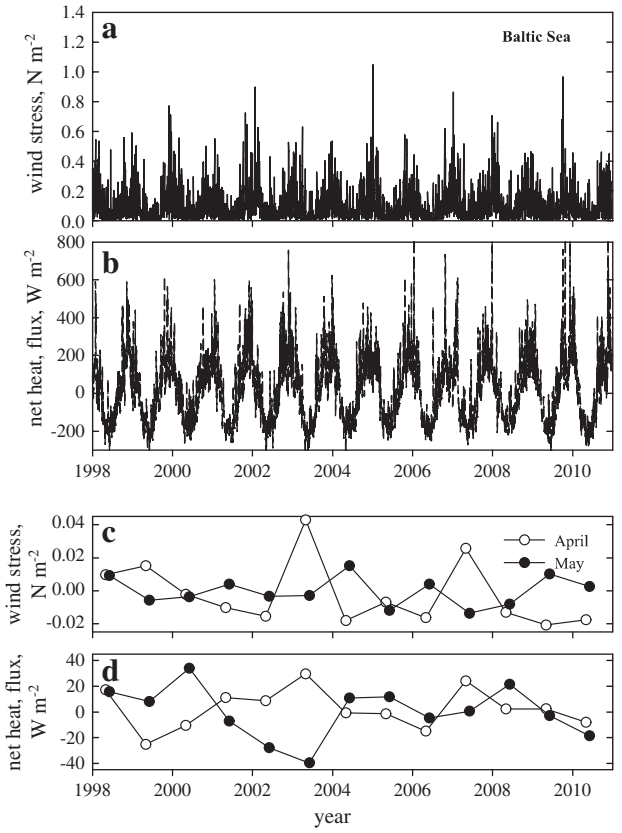

Fig. 5. Top panels: the 13-year time series of (a) wind stress magnitude and (b) net heat flux in the Baltic Sea study region. Bottom panels: monthly anomalies of (c) wind stress magnitude and (d) net heat flux in the months of April and May, calculated from time series shown in panels (a) and (b).

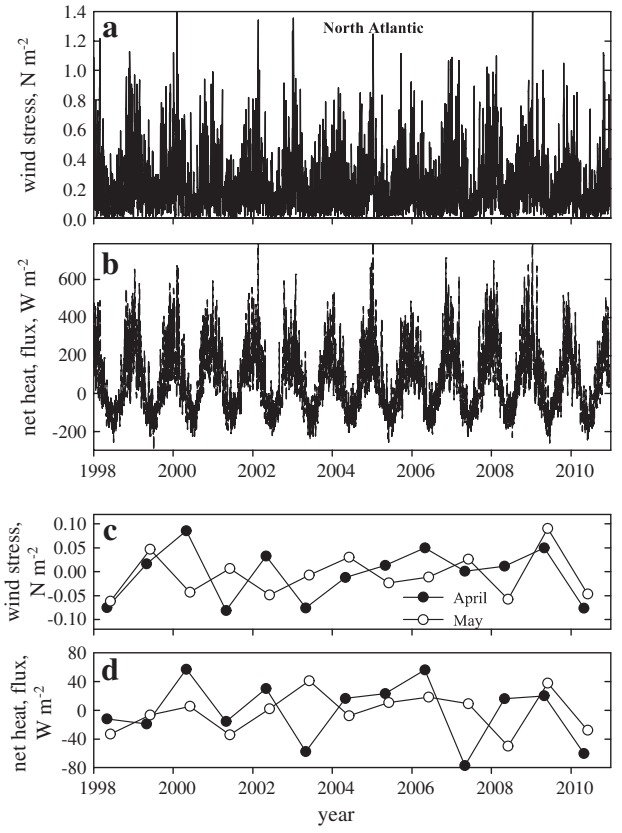

Fig. 6. Top panels: the 13-year time series of (a) wind stress magnitude and (b) net heat flux in the North Atlantic study region. Bottom panels: monthly anomalies of (c) wind stress magnitude and (d) net heat flux in the months of April and May, calculated from time series shown in panels (a) and (b).

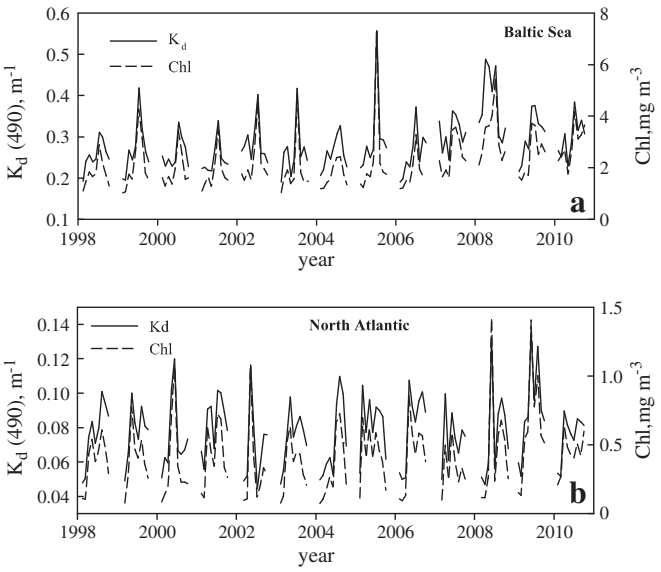

Fig. 7. The 13-year time series of monthly vertical attenuation coefficient $K_d(490)$ and monthly surface chlorophyll concentration (Chl) averaged in (a) the Baltic Sea study region and in (b) the North Atlantic study region.

as well as sufficient supply of nutrients from winter and early spring entrainment are conducive to very large growth of phytoplankton. At the selected North Atlantic site the highest Chl was observed in 2008 and 2009, while the lowest Chl was observed in 2010. In general, monthly time series of $K_d(490)$ and Chl displayed in Fig. 7a and b also indicate that in the North Atlantic site there is a better similarity between temporal patterns in $K_d(490)$ and Chl, than in the Baltic Sea region. Comparing Fig. 7a and b we also note that on average, Chl values are significantly higher in the Baltic Sea than in the open ocean waters of the North Atlantic. Such high Chl values are only possible as long as nutrients are replenished to the surface waters during the productive season. This can happen, for example, through mechanisms enhancing vertical mixing in the water column, nutrient recycling, and advection with terrestrial water (e.g., Moisander, Steppe, Hall, Kuparinen, & Paerl, 2003), but remote sensing data analyzed in this paper do not allow us to investigate these processes.

All the results presented below are similar if we used satellite-derived Chl or $K_d(490)$. We recognize that, in the future, more efforts are needed to fully validate or adapt the Chl GSM algorithm to the Baltic Sea before this algorithm can be used quantitatively. In contrast, $K_d(490)$ data product was extensively validated in the Baltic Sea in the past, based on large in situ data sets (Lee et al., 2005). This is why we have chosen to primarily present the results for the Baltic Sea using the $K_d(490)$ data product. Nevertheless, in the figure captions we also show the r^2 coefficients when Chl is used instead of $K_d(490)$. This is because, although the Chl GSM data product has not been fully validated in the Baltic Sea, comparisons with in situ data confirm that in situ patterns of temporal and spatial variability of Chl are well reflected in satellite Chl GSM data product (Coppini et al., 2012). Therefore, we decided that it might be interesting to show these results in a background. In the open ocean waters Chl and other satellite ocean color data products have been systematically validated (e.g., Bailey & Werdell, 2006). Note, that we do not include in our analysis the fall and winter seasons because of the limited availability of satellite ocean color data (or no data at all) in the region due to cloudy skies.

The results from the Baltic Sea indicate that the atmospheric variability as quantified by TKE_{RT}, wind stress, and net heat flux has minor effects on the interannual variability of ocean color in the Baltic Sea. The correlation coefficients between $K_d(490)$ (or Chl) and TKE_{RT}, wind stress, and net heat flux are statistically not significant (not shown). Only during the summer (July and August) we have found a positive correlation between the net shortwave radiation flux (NSWR) and $K_d(490)$ (Fig. 8). This is to be expected, since greater availability of sunlight supports more intensive growth of phytoplankton stock. The general lack of correlation between $K_d(490)$ (or Chl) and meteorological data (TKE_{RT}, wind stress, and net heat flux) seems somewhat surprising, because meteorological conditions are commonly considered as important factors influencing the interannual variability of phytoplankton blooms in the Baltic Sea (e.g., Leppäranta & Myrberg, 2009).

In contrast to the situation in the Baltic Sea, the results from our analysis for the North Atlantic site support the notion that atmospheric forcing plays a significant role for the development of phytoplankton blooms and interannual variability of ocean color in this region. The results from our analysis are similar to the findings described before for the north polar Atlantic, based on a shorter time series (Stramska, 2005). The current results based on the 13-year time series of $K_d(490)$ and Chl are briefly summarized in Fig. 9. The most noteworthy finding is the significant negative correlation between Chl (or $K_d(490)$) and TKE_{RT} in the spring (Fig. 9a). The net heat flux dominates the magnitude of TKE_{RT} during this time of the year, due to significant heat loss from the ocean to the atmosphere (compare Fig. 4). Wind stirring is also active and reinforces the effect of heat loss. Stronger mixing results in lower spatially-averaged surface Chl in April. This outcome is what one would expect for the early phase of the bloom, based on phytoplankton models (Doney et al., 1996; Fasham et al., 1990; Stramska & Dickey, 1994; Sverdrup, 1953). The rationale for this is that the very energetic atmospheric forcing has dramatic effects on redistribution of water properties in a weakly stratified ocean in the early spring. Increased mixing within the water column in April decreases phytoplankton growth, because average light energy available to phytoplankton cells becomes lower when the mixed layer is deepened. Mixing also increases phytoplankton losses because cells are removed from mixed layer into greater depth during the mixing events. As a result, in years with higher $TKE_{RT,}$ the spatially-averaged surface Chl in April is lower. Phytoplankton response to increased mixing in the North Atlantic in mid-to-late summer is different than in the early spring. Our analysis suggests that for both May and June the relationship between interannual variability of $K_d(490)$ (or Chl) and TKE_{RT} is not strong if considered on a monthly basis, although we did observe some negative correlation between Chl and TKE_{RT} in May (not shown). The cause for such a weak relationship during this time period can be explained as follows. Atmospheric forcing expressed by the magnitude of TKE_{RT} is much weaker in the May/June time period than it is in April. In addition, surface waters become more stratified and more energy is needed for significant deepening of *MLD*. As a result the mixing/restratification events are less intense in May/June than in April. Note also that, during this time period, increased mixing can have counteracting effects on phytoplankton: replenished nutrients allow for greater phytoplankton growth, while decreased average light energy received by phytoplankton cells decreases the growth rates. Thus, the main difference between April and May/June phases of the bloom in the North Atlantic is that in April there is no

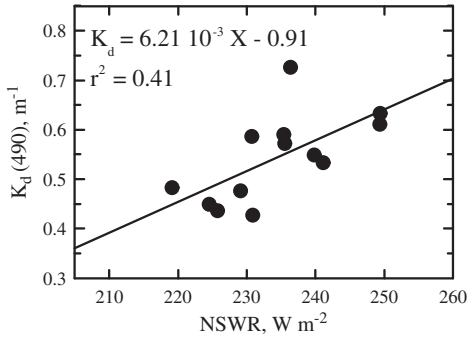

Fig. 8. Relationship between monthly vertical diffuse attenuation coefficient $K_d(490)$ and net shortwave radiation flux (NSWR) in the Baltic Sea in the month of July.

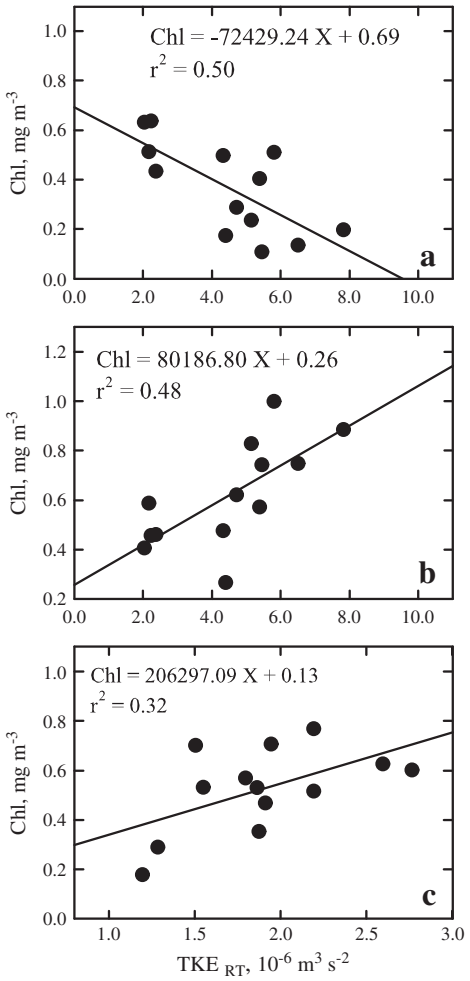

Fig. 9. Relationships in the North Atlantic between (a) monthly surface chlorophyll concentration (Chl) and turbulent energy generation rate (TKE_{RT}) in the month of April, (b) Chl averaged in May and June and TKE_{RT} in April, and (c) Chl and TKE_{RT}, both averaged over the 2-month period of July and August.

benefit to phytoplankton from mixing (because nutrients are plentiful anyway). What is more, mixing events can negatively influence phytoplankton growth (lower average light levels) and increase phytoplankton losses (transport to deeper, darker waters). As a result, we observe a strong negative correlation between Chl and TKE_{RT} in April, while the effects of atmospheric forcing on May/June Chl are not as evident. However, the interannual variability of Chl (and $K_d(490)$) averaged over the 2-month period of May and June showed significant positive correlation with the early spring values of TKE_{RT} (Fig. 9b). The interannual variability of Chl (and $K_d(490)$) averaged over a 2-month period of July and August is also sensitive to atmospheric forcing (Fig. 9c). The increase of mixing (or weaker stratification) during the summer due to higher TKE_{RT} is expected to have beneficial effects for sustaining a phytoplankton population, because it supplies nutrients and nutrients are most likely significantly limiting phytoplankton growth during this time period.

4.2. Rivers and variability of the vertical diffuse attenuation coefficient at 490 nm in the Baltic Sea

A summary of river data is provided in Fig. 10 as the 11-year averaged (1998–2008) time series of the daily total water discharge from the 75 largest rivers. These time series show that the interannual variability is significant. The annual cycle of the total discharge of water and nutrients by rivers is presented in Fig. 11 as the 11-year averaged time series of daily data. The 11-year averaged water discharge has a pronounced maximum in the spring (~at the beginning of May) with discharge about twice as high as the annual minimum discharge observed on average in late summer. The maximum discharge of nitrogen (N) and phosphorus (P) occurs, on average, prior to the maximum discharge of water. This is due to the fact that the total discharge of N and P is controlled by the rivers discharging into the Baltic Proper and in these rivers maximum annual water discharge happens earlier in spring than in rivers located more to the north.

The results from our analysis indicate that the river discharge has a dominant influence on the interannual variability of ocean color in the Baltic Sea. We found significant positive correlation between May and June $K_d(490)$ (and Chl) and the total water discharge into the Baltic Sea (January–May) (Fig. 12a and b). The correlation was even stronger if May $K_d(490)$ (or Chl) was plotted against nutrient discharge (Fig. 12c). These results are not quite unexpected, as it is well known that river discharge of freshwater has a fundamental influence on the Baltic Sea hydrography (Leppäranta & Myrberg, 2009). Nevertheless, it is for the first time that the link between river discharge and large scale ocean color variability in the open Baltic Sea has been documented.

The limited number of validated ocean color data products for the Baltic Sea makes a more in depth interpretation of our results somewhat difficult. Nevertheless, it is interesting to note that in May and June, we observed a very good correlation between $K_d(490)$ and the particulate backscattering coefficient $b_{bp}(443)$, as displayed in Fig. 13. Recall that the numerical values of K_d are, to the first approximation, equal to the sum of a and b_b (e.g., Mobley, 1994), with a in the eutrophic Baltic Sea waters being about an order of magnitude (or more) larger than the b_b. This means that the variability of K_d is driven mostly by changes in a. The significant relationship between K_d and b_{bp} shown in Fig. 13 reflects the strong correlation between bulk absorption and scattering properties of the Baltic surface waters in May and June. It is thus likely, that absorbing particles play a significant role in the variability of K_d described in this paper.

5. Summary and discussion

We have examined the interannual variability of ocean color in the Baltic Sea. Our results indicate that the influence of atmospheric forcing on interannual variability of $K_d(490)$ and Chl in the Baltic Sea is weak. This is in contrast to the North Atlantic, where the impact of atmospheric forcing on ocean color is quite significant.

In the North Atlantic our results are similar to the observations reported in the past for the north polar region of the Atlantic (Stramska, 2005). That is, in years with low TKE_{RT} the regionally-averaged $K_d(490)$ and Chl in April are higher than in years with elevated TKE_{RT}. This response of $K_d(490)$ and Chl to TKE_{RT} is also in agreement with phytoplankton models which predict development of blooms when mixing in the surface waters decreases significantly in comparison to the winter. During the May–June period, when regional TKE_{RT} is significantly lower than in April, the responses to

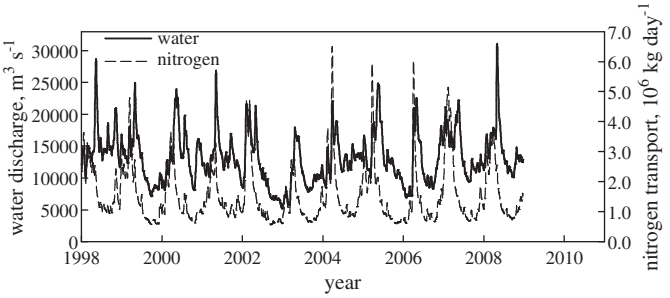

Fig. 10. The 11-year daily time series of the water, nitrogen, and phosphorus discharged into the Baltic Sea by 75 largest rivers.

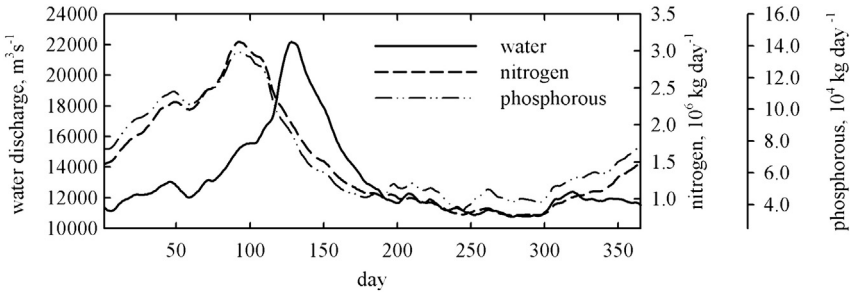

Fig. 11. The 11-year averaged daily time series showing an annual cycle in water, nitrogen, and phosphorus discharged into the Baltic Sea by 75 largest rivers.

meteorological conditions are not as strong. This is associated with opposite effects of enhanced mixing on phytoplankton population in the situation of moderate stratification of the water column. In this case an increase of mixing can increase phytoplankton growth when nutrients are needed, decrease growth if light energy becomes limiting, and intensify loss rates through removal of biomass from surface to deep waters. On the other hand, our data suggest that Chl averaged over May and June is influenced by the early spring (April) TKE_{RT}. In the July–August period nutrients are usually depleted, consequently meteorological conditions which favor lower water stratification supports higher Chl.

In the Baltic Sea we did not observe similar relationships between meteorological forcing and ocean color data. Only during the summer (July and August), there was a significant positive correlation between ocean color and net shortwave radiation (one of the components of the net heat flux). The discharge of freshwater and nutrients from rivers exerts more significant control on the interannual variability of $K_d(490)$ and Chl in the Baltic Sea than does the atmospheric forcing. In general, water transparency depends on (1) autochthonous production (the amount of plankton, detritus, etc. produced in the given region); (2) allochthonous materials (such as humic and minerogenic substances supplied to a given water body from outside sources, for example rivers); and (3) the amount of material resuspended from the sediment bed via wind/wave activity. Without access to more detailed information about the concentrations of different optically significant water components, we can only speculate about the possible reasons for the substantial correlation between river discharge and ocean color data. Maximum freshwater runoff occurs in April/May and coincides with the timing of the development of the phytoplankton spring bloom that is initiated by an increased stability and insolation of surface waters. Freshwater runoff contributes to the stabilization of the density structure of the water column, which can positively influence the intensity of the developing bloom. Importantly, river water carries a substantial load of dissolved inorganic nutrients. Availability of nutrients most likely enhances the phytoplankton bloom, which increases $K_d(490)$ and Chl. However, high concentrations of CDOM advected with river waters can also cause an increase in light attenuation. Finally, because with more river runoff the Baltic surface waters tend to be less salty, more stable, and more turbid, they also tend to warm more efficiently at the surface. This is because the vertical distribution of absorbed heat is different in waters with larger K_d (i.e., higher Chl, CDOM, and TSM concentrations)

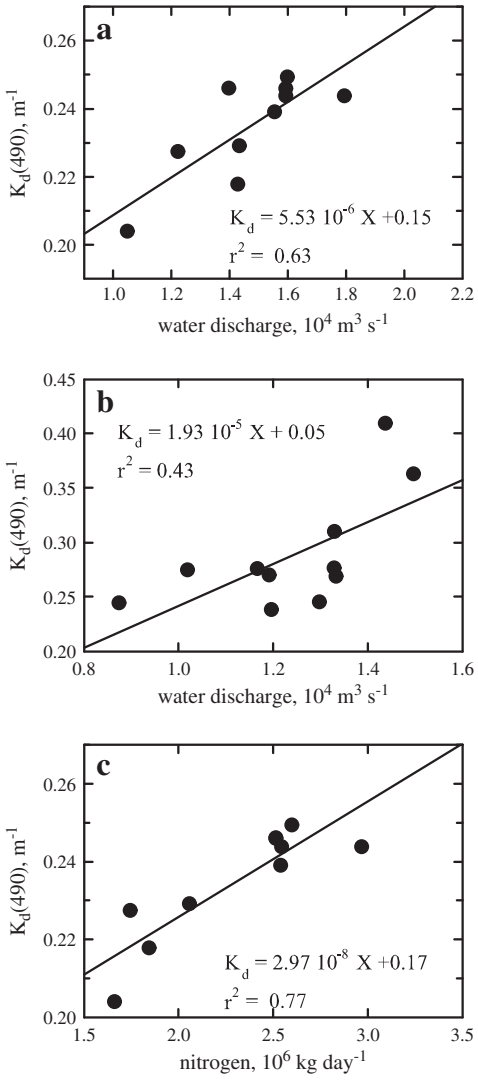

Fig. 12. Relationship in the Baltic Sea between (a) vertical diffuse attenuation coefficient $K_d(490)$ averaged in the study area in May and the total discharge of water from 75 largest rivers into the Baltic Sea averaged over the time period of January–May. (If Chl is used instead of $K_d(490)$ $r^2 = 0.42$), (b) the vertical diffuse attenuation coefficient $K_d(490)$ in June and the total runoff of water from the 75 largest rivers into the Baltic Sea, averaged over the time period of January–June. (If Chl is used instead of $K_d(490)$ $r^2 = 0.57$), (c) the monthly composite of the vertical diffuse attenuation coefficient $K_d(490)$ in May and the total nitrogen discharge from 75 largest rivers into the Baltic Sea, averaged over the time period of January–May. (If Chl is used instead of $K_d(490)$ $r^2 = 0.77$).

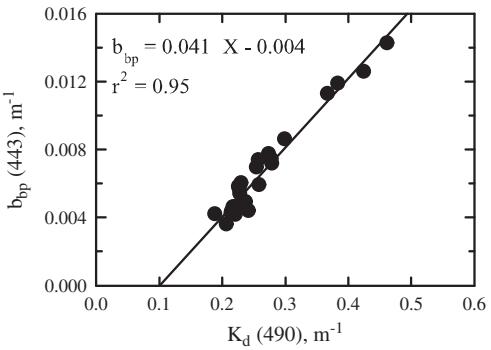

Fig. 13. Relationship between the vertical diffuse attenuation coefficient $K_d(490)$ and the backscattering coefficient $b_{bp}(443)$ averaged in the study area in the Baltic Sea in the months of May and June.

than in waters with lower K_d (e.g., Stramska & Zuzewicz, 2013). In addition, the heat delivered to the water surface from the atmosphere becomes entrapped in more stable surface layers (the vertical density gradient inhibits transfer of heat to deeper waters). Thus, the conditions for phytoplankton growth in years with larger river discharge can represent different water temperature, salinity, nutrient availability, and light fields than the conditions in years with lower river discharge. This in turn can have significant effects on the quantity as well as quality of the phytoplankton bloom.

In this paper we have discussed the interannual variability of the diffuse attenuation coefficient for downward irradiance in the Baltic Sea. The diffuse attenuation coefficient plays a critical role in many oceanographic processes. For example, K_d is essential for quantification of radiative heating of the ocean, in models of primary production and other photoprocesses, and in studies discussing water turbidity and water quality. Thus, the analysis of K_d variability in the Baltic Sea can lead to a better understanding of this marine environment. One of the important aspects of Baltic Sea research is the goal of remediating the eutrophication of this marine environment. This requires identification and understanding of environmental links responsible for variability of organic matter concentrations. The ultimate goal is to learn how to make educated predictions of how the given system would react to environmental and human induced changes. Our results strongly support the notion that such predictions, including those based on numerical models, must consider the interannual variability of river discharge. Note that currently, most numerical models include only the climatological average data on river discharge. Such models cannot be expected to simulate the interannual variability of the Baltic Sea ecosystem well.

One of our research objectives was to demonstrate that having an optical quantity (for example $K_d(490)$), which can be remotely derived, makes it possible to infer important geo-chemical information on a marine system. Our study documented that in the Baltic Sea the influence of the rivers on interannual variability of ocean color is more significant than the direct influence of atmospheric forcing. Note however that factors which were not included in our analysis can also influence ocean color and strength of phytoplankton blooms in the Baltic Sea. Such factors can include various biological processes such as grazing, mortality, and differences in composition of the phytoplankton population.

Acknowledgments

This work was supported through the SatBaltic project funded by the European Union through the European Regional Development Fund, (contract No. POIG.01.01.02-22-011/09 entitled 'The Satellite Monitoring of the Baltic Sea Environment'). The ocean color data were made available by NASA's Goddard DAAC and the SeaWiFS Science Project. The meteorological data were from the National Centers for Environmental Prediction and National Center for Atmospheric Research (NCEP/NCAR) Reanalysis Project provided by the NOAA/OAR/ESRL PSD, Boulder, Colorado, USA, from their Web site at http://www.esrl.noaa.gov/psd/. Mixed layer depth data were made available by C. de Boyer Montégut (www.ifremer.fr/cerweb/deboyer/mld). The river data were made available by the Swedish Meteorological and Hydrological Institute (www.balt-hypeweb.smhi.se/).

References

Babin, M., Stramski, D., Ferrari, G. M., Claustre, H., Bricaud, A., Obolensky, G., et al. (2003). Variations in the light absorption coefficients of phytoplankton, non-algal particles, and dissolved organic matter in coastal waters around Europe. *Journal of Geophysical Research*, *108*(C7), 3211. http://dx.doi.org/10.1029/2001JC000882.

Bailey, S. W., & Werdell, P. J. (2006). A multi-sensor approach for the on-orbit validation of ocean color satellite data products. *Remote Sensing of Environment*, *102*, 12–23.

Bergstrom, S., & Carlsson, B. (1994). River runoff to the Baltic Sea: 1950–1990. *Ambio*, *23*, 280–287.

Bricaud, A., Morel, A., & Prieur, L. (1981). Absorption by dissolved organic matter of the sea (yellow substance) in the UV and visible domains. *Limnology and Oceanography*, *26*, 43–53.

Coppini, G., Lyubarstev, V., Pinardi, N., Colella, S., Santoleri, R., & Christiansen, T. (2012). Chl a trends in European seas estimated using ocean-colour products. *Ocean Science Discussions*, *9*, 1481–1518. http://dx.doi.org/10.5194/osd-9-1481-2012.

de Boyer Montégut, C., Madec, G., Fischer, A. S., Lazar, A., & Iudicone, D. (2004). Mixed layer depth over the global ocean: An examination of profile data and a profile-based climatology. *Journal of Geophysical Research*, *109*, C12003. http://dx.doi.org/10.1029/2004JC002378.

Doney, S.C., Glover, D.M., & Najjar, R. G. (1996). A new coupled, one-dimensional biological–physical model for the upper ocean. Application to the JGOFS Bermuda Atlantic time series (BATS) site. *Deep Sea Research*, *43*, 591–624.

Donnelly, C., Strömqvist, J., & Arheimer, B. (2011). Modelling climate change effects on nutrient discharges from the Baltic Sea catchment: Processes and results. *Proceedings of symposium H04 held during IUGG2011 in Melbourne, Australia, July 2011, (IAHS Publ. 3XX, 2011)*.

Doron, M., Babin, M., Mangin, A., & Hembise, O. (2007). Estimation of light penetration, and horizontal and vertical visibility in oceanic and coastal waters from surface reflectance. *Journal of Geophysical Research*, *112*, C06003. http://dx.doi.org/10.1029/2006JC004007.

Ducklow, H. W., & Harris, R. P. (1993). Introduction to the JGOFS North Atlantic Bloom Experiment — The Joint Global Flux Study North-Atlantic Bloom Experiment. *Deep-Sea Research Part II*, *40*, 1–8.

Dutkiewicz, S., Follows, M., Marshall, J., & Gregg, W. W. (2001). Interannual variability of phytoplankton abundances in the North Atlantic. *Deep Sea Research*, *48*, 2323–2344.

Fasham, M. J. R., Ducklow, H. W., & McKelvie, S. M. (1990). A nitrogen-based model of plankton dynamics in the oceanic mixed layer. *Journal of Marine Research*, *48*, 591–639.

Fichot, C. G., Kaiser, K., Hooker, S. B., Amon, R. M. W., Babin, M., Belanger, S., et al. (2013). Pan-Arctic distributions of continental runoff in the Arctic Ocean. *Scientific Reports*, *3*, 1053. http://dx.doi.org/10.1038/srep01053.

Follows, M., & Dutkiewicz, S. (2002). Meteorological modulation of the North Atlantic spring bloom. *Deep Sea Research*, *49*, 321–344.

Friedrichs, M.A.M., et al. (2009). Assessing the uncertainties of model estimates of primary productivity in the tropical Pacific Ocean. *Journal of Marine Systems*, *76*, 113–133. http://dx.doi.org/10.1016/j.jmarsys.2008.05.010.

Fu, W., She, J., & Dobrynin, M. (2012). A 20-year reanalysis experiment in the Baltic Sea using three-dimensional variational (3DVAR) method. *Ocean Science*, *8*(5), 827–844.

Gordon, H. R., & Morel, A. (1983). *Remote assessment of ocean color for interpretation of satellite visible imagery — A review. Lecture notes on coastal and estuarine studies.* New York: Springer-Verlag.

Gregg, W. W. (2002). Tracking the SeaWiFS record with a coupled physical/biogeochemical/radiative model of the global oceans. *Deep-Sea Research II*, *42*, 81–105.

Håkanson, L., & Bryhn, A.C. (2008). Eutrophication in the Baltic Sea, present situation, nutrient transport processes, remedial strategies. *Series: Environmental Science and Engineering Series*New York: Springer-Verlag9783540709084.

HELCOM. (2009). Eutrophication in the Baltic Sea — An integrated thematic assessment of the effects of nutrient enrichment and eutrophication in the Baltic Sea region. *Baltic Sea Environment Proceedings*(No.115B) (148 pp.).

Hooker, S. B., & McClain, C. R. (2000). The calibration and validation of SeaWiFS data. *Progress in Oceanography*, *45*, 427–465.

IOCCG (2000). Remote sensing of ocean colour in coastal, and other optically-complex, waters. In S. Sathyendranath (Ed.), *Reports of the International Ocean-Colour Coordinating Group, No. 3, IOCCG, Dartmouth, Canada.*

IOCCG (2006). Remote sensing of inherent optical properties: Fundamentals, tests of algorithms, and applications. In Z. -P. Lee (Ed.), *Reports of the International Ocean-Colour Coordinating Group, No. 5, IOCCG, Dartmouth, Canada.*

Kirk, J. T. O. (1984). Dependence of relationship between inherent and apparent optical properties of water on solar altitude. *Limnology and Oceanography*, *29*, 350–356.

Kirk, J. T. O. (1991). Volume scattering function, average cosines, and the underwater light field. *Limnology and Oceanography*, *36*, 455–467.

Kowalczuk, P., Stedmon, C. A., & Markager, S. (2006). Modelling absorption by CDOM in the Baltic Sea from season, salinity and chlorophyll. *Marine Chemistry*, *101*, 1–11.

Kraus, E. B., Bleck, R., & Hanson, H. P. (1988). The inclusion of a surface mixed layer in a large-scale circulation model. In J. C. J. Nihoul, & B.M. Jamart (Eds.), *Small scale turbulence and mixing in the ocean* (pp. 51–62). Amsterdam: Elsevier.

Kraus, E. B., & Turner, J. S. (1967). A one-dimensional model of the seasonal thermocline, Part II: The general theory and its consequences. *Tellus*, *19*, 98–106.

Lee, Z. -P., Darecki, M., Carder, K. L., Davis, C. O., Stramski, D., & Rhea, W. J. (2005). Diffuse attenuation coefficient of downwelling irradiance: An evaluation of remote sensing methods. *Journal of Geophysical Research*, *110*, C02017. http://dx.doi.org/10.1029/2004JC002573.

Lee, Z. -P., Du, K. P., & Arnone, R. (2005). A model for the diffuse attenuation coefficient of downwelling irradiance. *Journal of Geophysical Research*, *110*, C02016. http://dx.doi.org/10.1029/2004JC002275.

Lee, Z. -P., Weidemann, A., Kindle, J., Arnone, R., Carder, K. L., & Davis, C. (2007). Euphotic zone depth: Its derivation and implication to ocean-color remote sensing. *Journal of Geophysical Research*, *112*, C03009. http://dx.doi.org/10.1029/2006JC003802.

Leppäranta, M., & Myrberg, K. (2009). *Physical Oceanography of the Baltic Sea. Springer-Praxis Book Series in Geophysical Sciences.* Chichester: Springer.

Maritorena, S., & Siegel, D. A. (2005). Consistent merging of satellite ocean color data sets using a bio-optical model. *Remote Sensing of Environment*, *94*, 429–440.

Maritorena, S., Siegel, D. A., & Peterson, A. (2002). Optimization of a semi-analytical ocean color model for global scale applications. *Applied Optics*, *41*, 2705–2714.

Marra, J. (2004). The compensation irradiance for phytoplankton in nature. *Geophysical Research Letters*, *31*, L06305. http://dx.doi.org/10.1029/2003GL018881.

Marra, J., Bidigare, R. R., & Dickey, T. D. (1990). Nutrients and mixing, chlorophyll and phytoplankton growth. *Deep Sea Research*, *37*, 127–143.

Marra, J., & Ho, C. (1993). Initiation of the spring bloom in the northeast Atlantic (47°N, 20°W): A numerical simulation. *Deep Sea Research*, *40*, 55–73.

Martin, P., Lampitt, R. S., Perry, M. J., Sanders, R., Lee, C., & D'Asaro, E. (2011). Export and mesopelagic particle flux during a North Atlantic spring diatom bloom. *Deep-Sea Research Part I*, *58*, 338–349. http://dx.doi.org/10.1016/j.dsr.2011.01.006 (ISSN 0967-0637).

Mikulski, Z. (1985). Water balance of the Baltic Sea. *Baltic Sea Environment Proceedings*, *16*, Helsinki: Helsinki Commission.

Mobley, C. D. (1994). *Light and water. Radiative transfer in natural waters*. New York: Academic Press.

Mobley, C. D., & Boss, E. (2012). Improved irradiances for use in ocean heating, primary production, and photo-oxidation calculations. *Applied Optics*, *51*, 6549–6560.

Moisander, P., Steppe, T. F., Hall, N. S., Kuparinen, J., & Paerl, H. W. (2003). Variability in nitrogen and phosphorus limitation for Baltic Sea phytoplankton during nitrogen-fixing cyanobacterial blooms. *Marine Ecology Progress Series*, *262*, 81–95.

Morel, A. (1988). Optical modeling of the upper ocean in relation to its biogenous matter content (case 1 waters). *Journal of Geophysical Research*, *93*, 10749–10768.

Nelson, N.B., & Siegel, D. A. (2002). Chromophoric DOM in the open ocean. In D. A. Hansell, & C. A. Carlson (Eds.), *Biogeochemistry of Marine Dissolved Organic Matter* (pp. 547–578). San Diego: Academic Press.

Neumann, T., Fennel, W., & Kremp, C. (2002). Experimental simulations with an ecosystem model of the Baltic Sea: A nutrient load reduction experiment. *Global Biogeochemical Cycles*, *16*, 1033. http://dx.doi.org/10.1029/2001GB001450.

Niiler, P. P., & Kraus, E. B. (1977). One-dimensional models of the upper ocean. In E. B. Kraus (Ed.), *Modelling and Predictions of the Upper Layers of the Ocean* (pp. 143–172). Oxford: Pergamon.

Omstedt, A., Elken, J., Lehmann, A., & Piechura, J. (2004). Knowledge of the Baltic Sea physics gained during the BALTEX and related programmes. *Progress in Oceanography*, *63*, 1–28.

Reid, P. C., Colebrook, J. M., Matthews, J. B.L., & Aiken, J. (2003). The continuous plankton recorder: Concepts and history, from plankton indicator to undulating recorders. *Progress in Oceanography*, *58*, 117–175. http://dx.doi.org/10.1016/j.pocean.2003.08.002.

Riley, G. A., Stommel, H., & Bumpus, D. F. (1949). Quantitative ecology of the plankton of the western North Atlantic. *Bulletin of the Bingham Oceanographic Collection*, *12*, 1–169.

Roesler, C. S., Perry, M. J., & Carder, K. L. (1989). Modeling in situ phytoplankton absorption from total absorption spectra in productive inland marine waters. *Limnology and Oceanography*, *34*, 1510–1523.

Siegel, D. A., Doney, S.C., & Yoder, J. A. (2002). The North Atlantic spring bloom and Sverdrup's critical depth hypothesis. *Science*, *296*, 730–733.

Siegel, D. A., Maritorena, S., Nelson, N.B., Hansell, D. A., & Lorenzi-Kayser, M. (2002). Global distribution and dynamics of colored dissolved and detrital organic materials. *Journal of Geophysical Research*, *107*, 3228. http://dx.doi.org/10.1029/2001JC000965.

Smetacek, V., & Passow, U. (1990). Spring bloom initiation and Sverdrup's critical-depth model. *Limnology and Oceanography*, *35*, 228–234.

Stramska, M. (2005). Interannual variability of seasonal phytoplankton blooms in the north polar Atlantic in response to atmospheric forcing. *Journal of Geophysical Research*, *110*, C05016. http://dx.doi.org/10.1029/2004JC002457.

Stramska, M., & Dickey, T. D. (1993). Phytoplankton bloom and the vertical thermal structure of the upper ocean. *Journal of Marine Research*, *51*, 819–842.

Stramska, M., & Dickey, T. D. (1994). Modeling phytoplankton dynamics in the northeast Atlantic during the initiation of the spring bloom. *Journal of Geophysical Research*, *99*, 10,241–10,252.

Stramska, M., Dickey, T. D., Plueddemann, A., Weller, R., Langdon, C., & Marra, J. (1995). Bio-optical variability associated with phytoplankton dynamics in the North Atlantic Ocean during spring and summer of 1991. *Journal of Geophysical Research*, *100*, 6621–6632.

Stramska, M., & Frye, D. (1997). Dependence of apparent optical properties on solar altitude: Experimental results based on mooring data collected in the Sargasso Sea. *Journal of Geophysical Research*, *102*, 15 679–15 691.

Stramska, M., Stramski, D., Mitchell, B. G., & Mobley, C. D. (2000). An inverse model for in-water optical measurements based on radiative transfer simulations. *Limnology and Oceanography*, *45*, 628–641.

Stramska, M., & Zuzewicz, A. (2013). Influence of the parameterization of water optical properties on the modeled sea surface temperature in the Baltic Sea. *Oceanologia*, *55*(1), 53–76.

Sverdrup, H. U. (1953). On conditions for the vernal blooming of phytoplankton. *Journal du Conseil International pour l'Exploration de la Mer*, *18*, 287–295.

Wozniak, B., Krezel, A., Darecki, M., Wozniak, S. B., Majchrowski, R., Ostrowska, M., et al. (2008). Algorithms for the remote sensing of the Baltic ecosystem (DESAMBEM). Part 1: Mathematical apparatus. *Oceanologia*, *50*, 451–508.

Zaneveld, J. R., Kitchen, J. C., & Pak, H. (1981). The influence of optical water type on the heating rate of a constant depth mixed layer. *Journal of Geophysical Research*, *86*, 6426–6428.